SPE 141462

Wettability Alteration and Foam Mobility Control in a Layered 2-D Heterogeneous Sandpack

Robert F. Li, George J. Hirasaki, and Clarence A. Miller, SPE, Rice University; and Shehadeh, K. Masalmeh, SPE, Shell Technology Oman

Summary

In a layered 2-D heterogeneous sandpack with a 19:1 permeability contrast that was preferentially oil-wet, the recovery by waterflood was only 49.1% of original oil-in-place (OOIP) due to injected water flowing through the high-permeability zone leaving the low-permeability zone unswept. In order to enhance oil recovery, an anionic surfactant blend (NI) was injected that altered the wettability and lowered the interfacial tension (IFT). Once IFT was reduced to ultra-low values, the adverse effect of capillarity retaining oil was eliminated. Gravity-driven vertical counter-current flow then exchanged fluids between high- and low-permeability zones during a 42-day system shut-in. Cumulative recovery after a subsequent foamflood was 94.6% OOIP even though foam strength was weak. Recovery with chemical flood (incremental-recovered-oil/waterflood-remaining-oil) was 89.4%. An alternative method is to apply foam mobility control as a robust viscous force dominant process with no initial surfactant injection and shut-in. The light crude oil studied in this paper was extremely detrimental to foam generation. However, the addition of lauryl betaine to NI at a weight ratio of 1:2 (NI : lauryl betaine), made the new NIB blend a good foaming agent with and without the presence of the crude oil. NIB by itself as an IFT reducing and foaming agent is shown to be effective in various secondary and tertiary alkaline/surfactant/foam (ASF) processes in water-wet 1-D homogeneous sandpacks, and in an oil-wet, heterogeneous layered system with a 34:1 permeability ratio.

Introduction

In a preferentially oil-wet, layered reservoir with large permeability contrast, the recovery factor is low because injected water sweeps only the high-permeability layer leaving the low-permeability layer unswept. When capillary communication is allowed between the two layers, water injected into the low-permeability zone will quickly bypass oil there by crossflowing into the high-permeability layer [Masalmeh and Wei, 2009].

In order to improve oil recovery in such a reservoir where the high-permeability layer lies above the low-permeability layer, it is desired to develop a chemical formulation that can alter the wettability from preferentially

oil-wet to preferentially water-wet, and/or reduce IFT such that the effect of capillarity retaining oil can be overcome and gravity-driven crossflow can exchange liquids between the layers. Spontaneous imbibition occurs when the wettability is altered to preferentially water-wet [Austad *et al.* 1997; Chen *et al.* 2000]. With IFT reduction, especially to ultra-low values, capillarity-induced spontaneous imbibition may be insignificant because capillary pressure may become negligible. However, buoyancy, independent of wettability, will lift oil upward and draw in injected chemicals to replace the oil that has been displaced, thereby becoming a dominant force [Hirasaki and Zhang, 2004]. If surfactant becomes depleted due to adsorption or dilution by connate water, diffusion may become an important factor [Masalmeh and Oedi, 2009].

The injected chemicals can be introduced into the lower permeability zones not only by spontaneous imbibition or the above mechanism, but also by foam that diverts the liquid into the lower permeability layer [Li *et al.*, 2010]. Foam mobility control can also in this way improve sweep efficiency. Since first introduced in a laboratory study of surfactant flooding three decades ago [Lawson and Reisberg 1980], foam as a mobility control agent has been successful in many field applications such as in steam foam flood [Hirasaki 1989; Patzek 1996], foam assisted water alternating gas injection in the Norwegian Snorre field [Blaker *et al.* 2002], aquifer remediation [Hirasaki *et al.* 1997-2000], alkaline/surfactant/polymer (ASP) flooding [Wang *et al.* 2001], etc. One of the unique attributes of foam in layered systems that makes foam more favorable than polymers is that foam has higher apparent viscosity in high- than in low-permeability layers and therefore improves sweep [Heller 1994; Bertin *et al.* 1999; Kovscek and Bertin 2003; Nguyen *et al.* 2005]. It has been shown in a layered 2-D system with 19:1 permeability contrast with inter-layer capillary communication that foam diverted surfactant solution from the high-permeability layer to the low-permeability layer. Ahead of the foam front, liquid in the low-permeability layer crossflowed into the high-permeability layer [Li *et al.* 2010].

For a given surfactant and oil system, it is commonly observed that strong foam is generated at salinities far below optimum. However, IFT is minimized near optimal salinity. This leads to a dilemma that a surfactant formulation that can reduce IFT to ultra-low values is not a good foaming agent, and vice versa. As a consequence, in such a flooding process, foam is usually injected as a drive after the low-tension surfactant slug [Li *et al.*, 2010]. The disadvantage of this scheme is that the low-tension surfactant slug is lacking mobility control, leading to poor sweep. It is ideal to develop a single surfactant formulation that can simultaneously reduce IFT to ultra-low values and generate strong foam so that microscopic displacement as well as sweep efficiency will be greatly improved from the beginning of the chemical flooding process.

It is well-known that crude oils often destabilize foam and widely believed that light crude oils are more effective defoaming agents. The mechanisms have been extensively investigated [Garrett 1993; Aveyard 1994; Zhang *et al.* 2003; Schramm 2005]. Garrett summarized three coefficients, namely the entry coefficient E, the spreading coefficient S, and the bridging coefficient B, that are important in interpreting the mechanisms of oil destabilizing foam. These coefficients are defined as follows:

where, stand for air/water, oil/water, and air/oil interfacial tensions. To break a foam lamella, an oil drop must enter the air/water surface, *i.e.* $E>0$. In order to enter the air/water surface, the oil drops must first overcome the repulsive forces caused by the pseudoemulsion films separating these drops from the air/water interface [Nikolov *et al.* 1986; Manlowe and Radke 1990]. Once an oil drop enters, it may spread at the air/water interface *i.e.* $S\geq 0$, leading to foam lamella rupture. When $S\leq 0$ an oil drop forms a lens on one side of the air/water interface and may reach the other side as the foam film thins, thus forming a bridge. If $B>0$, the bridge is unstable and the film breaks. By understanding these mechanisms, surfactants that can stabilize foam in presence of oil – foam 'boosters' – can be designed. Betaine surfactants are used commercially as foam boosters in the detergent industry. The mechanism of stabilizing foam may be due to increasing the critical capillary pressure for the stability of the pseudoemulsion film [Basheva, *et al*., 2000].

In this paper, we will first experimentally demonstrate a process with surfactant induced wettability alteration and gravity drainage in improving oil recovery in a preferentially oil-wet, layered, 2-D model with a 19:1 permeability contrast. Next, foam as an alternative to improve recovery in a similar system is discussed. We focused on analyzing the adverse effects of the crude oil that destabilized the foam and have developed surfactant foaming formulations with the addition of a betaine surfactant that are tolerant to the crude oil. Furthermore, we have optimized a single surfactant formulation that can reduce IFT to low values and generate foam for mobility control at the same time. The formulation has shown successful performance in 1-D, water-wet, homogeneous sandpacks in secondary or tertiary recovery processes as well as in a preferentially oil-wet, heterogeneous, layered system in a tertiary recovery process.

Experimental Procedure

Materials. The materials used in this paper are summarized in **Table 1**.

Equipment

Surface Properties Determination. The zeta potential of clean and CTAB-treated silica flour was measured by Beckman Instrument Coulter DELSA 440 (conductivity 2.37~2.46 mS/cm, 1% wt solid in 0.02 mol/L NaCl). An Olympus SZX12 stereo microscope equipped with a camera was used in taking microscopic pictures on the pore level. Water receding and advancing contact angles were measured by KSV Instrument with CAM2008 software. [Treiber et al. 1972; Hjelmeland et al. 1986; Yang et al. 2000]. Three types of microscopic glass slides with different surface properties were used***,*** as listed in **Table 2**. The water receding contact angle was measured when the contact line between the glass surface and the oil drop appeared at equilibrium after about 5 minutes. In order to measure the water advancing contact angle, the same drop of oil on the glass was carefully withdrawn stepwise by a small but noticeable volume. If the contact line changed within 5 minutes, the water advancing contact angle was recorded, otherwise, another step size of oil was withdrawn. IFT between crude oil and brine was measured using the pendant drop method. IFT between crude oil and surfactant solution (NI) was measured using the spinning drop method with a University of Texas model 300 spinning drop tensiometer.

Column Sandpack. The 1-D system was a 1-ft-long glass column with 1-in. inner diameter tightly packed with silica sand. The heterogeneous column was packed using a 1-in. thin metal strip inserted in the center to separate coarse and fine sands. The metal strip was removed at the end of packing. The experimental set up can be referred to in a recent published paper in SPE Journal [Li *et al.*, 2010]. All experiments were conducted at ambient room temperature.

2-D Heterogeneous Sandpack. The 2-D system was made of stainless steel with a 1.25-in. thick glass observation window in the front. The interior was a 20×3×0.75-in. chamber. **Fig. 1** is a photograph of the 2-D sandpack saturated with water. Arrows show direction of flow through manifolds. The experimental set up can be referred to in a recent published paper in SPE Journal [Li *et al*., 2010]. The model was packed with two layers of silica sand, high permeability coarse sand Oil Frac 20/40 on top and low permeability fine sand F-110 on bottom. For the top (Oil Frac 20/40) and bottom (F-110) layers, the thickness ratio was 2:3 and the permeability ratio was 19:1 (90 and 4.8 darcy, measured individually in 1-D homogeneous sand columns). The total pore volume (TPV) was 330 mL. The overall porosity was 0.38, and the measured overall permeability was 44 darcy. Overall permeability was measured by injecting water at a constant rate through a manifold, as shown in Fig. 1. Pressure drop across the entire sandpack was measured. Overall permeability was then calculated using Darcy's law. Notice the discrepancy in overall permeability between the measured value (44 darcy) and the theoretically

calculated value (39 darcy). This may have been due to sand in 2-D model was not as tightly packed as it was in 1-D columns.

All sandpacks were saturated with brine before oilflood unless otherwise stated. Flow direction in vertical 1-D homogeneous sand columns was from bottom to top, and was from left to right in photographs of horizontal heterogenous 1-D and 2-D sand packs presented below.

Results and Discussion

Surfactant Induced Wettability Alteration and Gravity Drainage EOR Processes in a 2-D Oil-Wet Heterogeneous Sandpack. In a preferentially oil-wet heterogeneous reservoir with large permeability contrast, the recovery was low due to injected water flowing through the high-permeability zone leaving the low-permeability zone unswept [Masalmeh and Wei, 2009] To enhance oil recovery, a surfactant formulation *i.e.* NI, was developed which altered the wettability and lowered the IFT. Consequently the effect of capillarity retaining oil was eliminated due to negligible capillary pressure, and gravity driven counter-current flow exchanged fluids between high- and low-permeability zones. The measured IFT between SME crude oil and 2% (wt) NaCl brine was 26.5 mN/m. Between two batches of crude oil sample received, the IFT values between SME and 0.2% NI were below about 0.01 mN/m (in 2% NaCl, 1% Na_2CO_3) and no greater than 0.002 mN/m (in 3.5% NaCl, 1% Na_2CO_3 and 4.15% NaCl, 1% Na_2CO_3). However when NaCl was greater than 4%, surfactant precipitation occurred. The surfactant formulation of NI in either 2% or 3.5% NaCl, with 1% Na_2CO_3 was adopted in the following experiments for a clear single phase solution. **Table 3** summarizes the process.

Surface Treatment with CTAB. Silica sands in the 2-D model were treated to be oil-wet by ½ CMC CTAB solution. CTAB could effectively alter the wettability of clean silica surface from preferentially water-wet to preferentially oil-wet. Furthermore the wettability of CTAB-treated surface could be altered back to preferentially water-wet in the presence of anionic surfactants *e.g*. NI. Zeta potential measurements showed CTAB-treated silica flour surface was positively charged (29.2 mV), compared to negatively charged untreated clean silica surface (-53.9 mV). **Fig. 2** shows water receding and advancing contact angle measurements on various glass surfaces. When $0°<\theta<75°$ a surface is preferentially water-wet, and when $115°<\theta<180°$ it is preferentially oil-wet, where θ is the contact angle measured through the water phase [Morrow 1990]. From these measurements, it is concluded that CTAB was able to effectively change the wettability of glass surface from preferentially water-wet to preferentially oil-wet. Anionic surfactants such as NI could alter the wettability of CTAB-treated glass from preferentially oil-wet back to preferentially water-wet. The mechanism of wettability alteration in this paper can be

related to the mechanisms observed in oilfield formation rocks. It is reported that injected cationic surfactants were able to alter the wettability of low permeability chalk cores from oil-wet to water-wet by desorbing carboxylates from the chalk surface and consequently oil was recovered by spontaneous imbibitions [Standnes and Austad, 2000]. The mechanism lies in formation of ion pairs between the cationic surfactants and adsorbed negatively charged carboxylates in the oil. Similarly, in our experiments, the injected anionic surfactant *i.e.* NI desorbed CTAB from the sand surface by forming ion pairs and altered the wettability from oil-wet back to water-wet.

Oilflood and Waterflood. After the sands were treated with CTAB and purged with sufficient 2% NaCl brine, oilflood was carried out by injecting SME crude at 5-10 ft/D through various ports located at the side and the back of the sandpack. Oil saturation after oilflood was 62.4%. Remaining water (brine) saturation was 37.6%, much higher than the irreducible water saturation. Due to the 19:1 large permeability contrast between high and low layers, injected oil flowed mainly in the upper high permeability layer. Also due to the limited quantity of crude oil sample, we were unable to carry out the oilflood long enough to reach the actual irreducible water saturation in the entire sandpack. **Fig. 3** shows a photograph of the sandpack after oilflood. Next, the 2-D sandpack was waterflooded using 2% NaCl at 5ft/D (~0.06 psi/ft). **Fig. 4** shows a photograph at the end of waterflood. After 4.0 PV, the lower layer still remained highly oil-saturated while the oil-cut from the effluent had already been near zero. Waterflood recovered 49.1% OOIP. Remaining oil saturation was 31.8%. As a comparison, if the sandpack was water-wet, waterflood displaced much more oil from the lower tight layer by spontaneous imbibitions than if it was oil-wet [Li, 2011].

Surfactant Induced Wettability Alteration and Gravity Drainage. NI was injected at 1 ft/D for a total of 0.5 PV. It broke through in the top layer between 0.4 and 0.5 PV. The first photo in **Fig. 5** was taken immediately after the NI flood. The lower layer, however, still remained highly oil-saturated due to unfavorable mobility. This process alone recovered only 2.3% OOIP. Oil saturation after this process was 30.3%.The system was then shut in for 42 days. Fig. 5 shows photographs taken during this settling process. Streaks of oil were observed immediately in the upper layer upon shut-in. Also, streaks of upward-moving oil were observed on day 5 in the lower layer. A rim of oil had accumulated on top of the sandpack. Note that the patch of oil near the inlet changed slowly compared to other locations in the lower layer. This may have been due to water-in-oil emulsion already present in this portion of the injected oil, which may have increased the viscosity and density. The emulsion was not formed *in-situ* during the flooding processes but was brought in by injected oil that might have contained emulsion during oilflood. This is because many PV's of oil were required to flood the entire sandpack with its large permeability contrast. Due to the limited quantity of the crude sample, oil from the effluent of these oilflooding

cycles was separated from brine and re-injected. Insufficient time during separation by centrifuging of one portion of the crude oil may have caused this water-in-oil emulsion.

Although the permeability values of both layers were much higher than real reservoir rocks, the vertical extent in the sandpack under study was small as well. Thus, the capillary transition length was significant in this system [Dake, 1978]. In addition, oil in smaller pores in the lower tight layer had lower relative permeability even if it was mobile. Buoyancy would have lifted up remaining oil from the lower tight layer. However, capillarity, because of the oil-wet nature, retained oil in that region. Then injected NI reduced the IFT between oil and brine by three orders of magnitude and therefore dramatically reduced the capillary pressure. As a result, the capillarity retaining effect became very small, allowing buoyancy to lift untrapped oil upward. Simultaneously, surfactant solution flowed downwards to replace the oil that had floated upwards, which resulted in further contact with oil at reduced IFT. This process dramatically displaced most of the remaining oil from the lower tight layer.

The data were interpreted by evaluating the effects of gravity drainage and capillarity. The dimensionless time for gravity drainage alone assuming zero capillary pressure was defined as follows [Richardson and Blackwell, 1971; Hagoort, 1980]:

(4)

Relative permeability was estimated by the Corey correlation

(5)

In this equation, =0.9 and a Corey exponent of =3 were used.

The dimensionless time for capillary imbibition assuming zero gravity was defined as follows [Ma *et al.*, 1997],

(6)

These dimensionless times were indicated in Fig. 5. **Fig. 6** shows plots of recovery as a function of dimensionless time for gravity , and for capillary pressure . The experiment was compared with the 1-D analytical solution for gravity drainage [Richardson and Blackwell, 1971; Hagoort, 1980].

(7)

The experiment recovered oil much slower than gravity drainage alone (assuming zero capillary pressure). This is because, at the beginning of system shut-in, surfactant was not present in the entire lower layer, and areas where surfactant had not yet reached were still oil-wet. The adverse capillary pressure dominated gravity and retarded recovery by buoyancy. Once surfactant came in contact with oil, the tension was reduced to an ultra-low

value and the capillarity became negligible compared to gravity. Then buoyancy force became dominant and contributed significantly in displacing oil which had been contacted with surfactant. Another reason that could account for the recovery being much slower than expected for gravity drainage is the delay in getting low IFT and/or wettability change well down into the lower layer. In the first place, the pore volume of the lower tight layer was approximately 50% greater than that of the upper coarse layer. Also NI may have been lost to the process by combining with desorbed CTAB to form ion pairs, some of which likely dissolved in the oil as proposed by Standnes and Austad (2000). Some desorbed CTAB or some ion pairs may have also entered the microemulsion droplets or other aggregates and shifted phase behavior to be more lipophilic. The desorption of CTAB and its combination with anionic surfactants would result in the delay in getting NI to the bottom of the lower layer.

As a comparison, if surfactant solution was present everywhere from all sides, the rate limiting step would be gravity. This has been observed in the spontaneous imbibition test in an Amott cell [Hirasaki and Zhang, 2004]. In that test, the oil-saturated core sample was surrounded by surfactant. Surfactant solution entered from the sides and the bottom and promoted a co-current upward flow of both phases. The recovery took place around t_{Dg}=1, and agreed fairly well with the analytical solution. Similar surfactant-induced co-current flow processes were also discussed by Gupta and Mohanty (2007). It should be noted that the co-current flow model is close to what happened in an Amott cell in which gravity effects dominated than in this particular 2-D experiment. In this 2-D experiment, gravity also drove the flow but flow was counter-current and there was no stable displacement front. Even though the co-current flow analysis was not especially representative of our situation, the choice of definition of dimensionless time may be.

This 2-D experiment is different than the spontaneous counter-current imbibition process in a very strong water-wet (VSWW) system assuming zero gravity, as shown by the purple curve [Aronofsky *et al*., 1958] in Fig. 6. This is because in the 2-D experiment: 1) the system was not water-wet but rather, preferentially oil-wet, which resulted in negative capillary pressure that retained oil; and 2) gravity was a driving force and therefore displacement was faster than if capillary pressure solely dominated. In this experiment, P_c was nearly zero where surfactant was present, and P_c was still negative (oil-wet) where surfactant had not reached. Therefore, the rate limiting step of this process was the transport of surfactant solution to the trapped oil, *i.e.* how fast the front of P_c=0 advanced. This phenomenon was evident from the profiles in Fig. 5, especially day 6 and day 10 after shut-in. Streaks of oil at low tension floated up by buoyancy above the front of the surfactant solution displacing remaining oil. Below the front, oil at high tension was still trapped.

After the shut-in, foamflood using SAG injection scheme was conducted with gas fractional flow *fg*=1/3 and a gas slug size of 0.1 PV at ~1.6 psi/ft. **Fig. 7** shows the photographs during the foamflood. As soon as IOS 15-18 was injected, remaining oil in the lower layer near the inlet was mobilized**.** **Fig. 8** shows that foam apparent viscosity oscillated between about 1 and 4 cp over each cycle of gas and liquid injection. Strong foam was not formed. This may have been due to high oil saturation in the top layer breaking the foam. The patch of oil which had been difficult to displace during shut-in was mobilized during the foamflood. Furthermore, it continued moving upwards after the foamflood, when counter-current flow between oil and aqueous phase immediately resumed (**Fig. 9**). The top photo in Fig. 9 was taken 1.5 hours after the end of the foamflood; the bottom was taken 4 days afterwards. **Fig. 10** is a photo of effluent samples from the foamflood. It shows that most oil was recovered within 1.1 TPV of the foamflood, and oil-cut was substantial. The foamflood in addition to the earlier alkaline surfactant flood recovered 89.4% of the waterflood remaining oil. Overall recovery (waterflood+ASF) was 94.6% of OOIP. Oil saturation after this point was reduced to only 3.4%. **Fig. 11** is a plot of cumulative recovery. Recoveries would have been higher except for inadvertent injection of emulsion near entrance of the bottom layer.

Foam Mobility Control in Presence of SME Crude. So far, we have demonstrated that surfactant induced wettability alteration and IFT reduction can greatly improve oil recovery in an oil-wet heterogeneous system with 19:1 permeability contrast. An alternative method is to apply foam mobility control as a robust viscous force dominant process. The crude oil studied in this paper was a light crude (API=41.1°), and was extremely detrimental to foam stability. We have shown that NI can reduce IFT to ultra-low values, but it was a weak foaming agent even in the absence of crude oil. However, with the addition of lauryl betaine, a zwitterionic surfactant, at a weight ratio of 1:2 NI:B, the new NIB formulation became a good foaming agent (**Fig. 12**).

The micro model picture shown in **Fig. 13** reveals that NI, being a weak foaming agent, did not stabilize foam lamellae in presence of SME. Air flowed in continuous gas channels. However, **Fig. 14** shows that NIB could stabilize foam lamellae. Trapped gas flowed as bubble chains even in the presence of oil, resulting in gas mobility reduction. The dark color on the contour of a bubble or a bubble chain indicates oil was in very close proximity to bubbles but did not break them. Since oil drops did not form lenses or rupture foam lamellae, it is possible that these drops could not reach the air-water interface through a pseudoemulsion film or could not enter the interface if they did reach it, *i.e., E≤0* [Basheva, *et al*., 2000].

All experiments described below were ASF EOR processes at ambient temperature without using polymer. Foam in presence of oil was first evaluated in water-wet, 1-D homogeneous sandpacks, then in a layered, oil-wet heterogeneous sand column with a permeability ratio of approximately 34:1.

Foam as a Drive in Presence of Oil in Water-Wet 1-D Homogeneous Sandpacks. The initial condition was waterflood residual oil condition. Foam as a drive was generated by surfactant alternating air (SAG) injection at constant pressure gradient (1.2 ~1.4 psi/ft). IOS 15-18 was a strong foaming agent in the absence of oil but could not generate foam in presence of SME crude. Two experiments are compared below. Experiment (a) had no betaine in either NI slugs or IOS 15-18 slugs in the foam drive. Experiment (b) had lauryl betaine in both NIB (NI and lauryl betaine blend) and IB (IOS 15-18 and lauryl betaine blend) whose individual blending ratio was optimized. These experiments are summarized in **Table 4** and **Figs. 15-20**.

The two experiments showed more rapid cumulative recovery of residual oil (Fig. 15) and increased foam apparent viscosity (Fig. 16) when we added lauryl betaine to NI and IOS 15-18 at the optimized ratios. Experiment (a) did not contain any betaine in either NI or IOS 15-18 slugs. There was not a distinctive oil bank and gas broke through the column early (Fig. 17). Recovery was slow (Fig. 15). Foam did not form due to the adverse effect of crude oil, and foam apparent viscosity was low (Fig. 16). All these results indicate that there was not effective mobility control. In experiment (b), we optimized the weight ratio between IOS 15-18 and lauryl betaine to be 10:1 in IB and 1:2 between NI and B in NIB. The 10:1 ratio was so chosen because this IB blend had the highest viscosity while still remaining as a clear single-phase solution (Fig. 19). This viscosity increase may be due to a sphere to rod micelle transition [Christov, *et al*., 2004]. The 1:2 ratio in NIB was chosen because qualitative foam bottle tests (Fig. 20) showed that foam with this ratio was stable both with and without crude oil while minimizing the use of lauryl betaine. The NIB blends did not display significant viscosity dependence on blending ratio. With both NIB and IB optimized, we see a distinctive oil bank forming and moving along the sandpack (Fig. 18). Foam did not break through the oil bank until 0.8 TPV as liquid fraction in the effluent (Fig. 18) remained nearly 100%. Most residual oil was recovered by 1.0 TPV, and oil recovery was more rapid than experiment (a). Foam apparent viscosity increased by an order of magnitude (Fig. 16). All these results indicate that foam worked well as an effective mobility control agent. The apparent viscosity and hence mobility ratio are important in sweeping a heterogeneous formation. When scaling up to a field application, the apparent viscosity should be chosen such that it is high enough to obtain a favorable mobility ratio yet not too high to cause injectivity problems.

NIB as One Formulation to Reduce IFT and Generate Foam for Mobility Control. NIB by itself in a tertiary recovery process was evaluated as shown in **Figs. 21-24**. Fig. 21 shows that there was a distinctive oil bank, and

its oil was recovered within 1.1 TPV. It also shows that gas did not break through the oil bank as the liquid fraction in the effluent was nearly 100% during this period. Cumulative recovery of waterflood residual oil was 97% (Fig. 22). Although foam was much stronger after most of the oil was displaced (Fig. 23), it still had higher viscosity than other surfactant formulations that had no betaine added. Injection rate was greatly reduced (Fig. 24) once foamed was generated, indicating favorable mobility.

The formulation was then evaluated in a secondary recovery experiment **Figs. 25-26**. Foam was not as strong as in the tertiary recovery case. This may have been due to the fact that oil saturation was much higher and it broke the foam. However, the cumulative recovery after 1.8 TPV was 99.6% of OOIP.

The oil bank observed during 0-0.2 TPV NIB injection in displacement profiles in Figs. 21 and 25 was a result of low IFT between SME and NIB. It happened during the first two slugs of NIB injection at a constant rate of 5 ft/D. There was a clearly defined oil bank below which the residual oil saturation was near zero as the sand below the oil bank appeared to be the same color as clean silica sand. IFT can be estimated using a dimensionless trapping number which combines the capillary number and the bond number [Pope *et al.*, 2000]. The simplified trapping number in these 1-D homogeneous sandpacks becomes

———— (8)

For example, in the experiment shown in Fig 21, the permeability was 174 darcy; =9.8 m/s^2 is the gravitational acceleration constant; the density difference was 288 kg/m^3; the pressure gradient was 908 Pa/m (0.040 psi/ft). In order to reach near zero residual oil saturation, needs to be greater than 10^{-3}. Consequently, IFT should be lower than 0.6 mN/m. The gravity term in this equation was more than three times as large as the pressure gradient . Buoyancy and high permeability can contribute to the displacement of trapped oil.

Gravity also improved sweep efficiency during early stage low-rate injection at 5 ft/D. A dimensionless gravity number in this 1-D experiment can be expressed as

—— (9)

where the oil viscosity was 3.93 cp. During 0-0.2 TPV, only NIB was injected at a low rate of 5ft/D. The calculated N_g=7.0 is greater than unity, which indicates that, regardless of mobility ratio, a piston-like displacement front will always result [Hirasaki, 1975]. It accounts for the gravity-stabilized well defined oil-banks at low TPV in Figs. 21 and 25. Starting from 0.3 TPV, fluid was injected at a constant pressure gradient (1.4 psi/ft), and the injection rate was very high before strong foam was formed (Fig 24). At 0.3 TPV (air injection) and 0.4 TPV (NIB injection), the rates were 382 ft/D and 340 ft/D, respectively. The dimensionless gravity number N_g was

determined to be 0.09 and 0.10, respectively. N_g<<1 and slightly unfavorable mobility ratio explain the tailing effect behind the oil bank after 0.3 TPV in Fig 21.

Foam Mobility Control in the Presence of Oil in an Oil-Wet Heterogeneous Layered System. NIB alone was evaluated in a horizontal layered, CTAB-treated, oil-wet silica column. Results are summarized in **Table 5** and **Figs. 27-29**. The vertical stripes in the upper layer are due to packing defects. After waterflood, oil saturation in lower layer remained high, judging from the color in Fig. 27. Viscous forces (by waterflood) or gravity could not overcome capillarity (oil-wet). As a result, capillarity retained most of oil in the lower tight layer. If the sandpack was water-wet, during water-flood, most remaining oil in the lower tight layer could be displaced by spontaneous imbibitions, as was experimentally demonstrated [Li, 2011]. Instead of shutting in the system after surfactant injection to let surfactant-induced wettability alteration and gravity drainage take place, we applied foamflood using NIB SAG immediately after waterflood as a viscous force controlling process. In this case, however, we had not tested whether or not NIB could alter the wettability of CTAB-treated silica from oil-wet to water-wet. NIB was a good foaming agent in presence of SME owing to betaine that stabilized pseudoemulsion films. Thus foam was formed and worked effectively as a mobility control agent in displacing remaining oil from the lower tight layer. The reduction in oil saturation is illustrated in Fig. 28 by noticeable color change in the lower layer. Cumulative recovery including waterflood and EOR recovered 93.1% OOIP. Fig. 29 is a plot of foam apparent viscosity. Foam kept building up and its apparent viscosity increased as injection continued.

Conclusions

1. CTAB was effective in altering the wettability of clean silica sand from water-wet to preferentially oil-wet. Anionic surfactants such as NI could alter the wettability back to preferentially water-wet.

2. A 2-D heterogeneous sandpack with a 19:1 permeability contrast was made preferentially oil-wet. Gravity-driven, vertical, counter-current flow occured after 0.5 PV alkaline/surfactant was injected and the system was shut-in. The effect of capillarity retaining oil was virtually eliminated once IFT was reduced to ultra-low values. This process displaced most of the oil from lower, low-permeability layer. Foamflood recovered most of the oil accumulated at the top of the high-permeability layer. Strong foam was not formed due to crude oil breaking the foam. Foamflood in addition to alkaline surfactant flood recovered 89.4% of the waterflood remaining oil. Overall recovery (waterflood+ASF) was 94.6% OOIP.

3. NI alone is not a good foaming agent. The addition of lauryl betaine made NIB a strong foaming agent with and without SME crude oil. NIB (NI:B=1:2) worked well in both secondary and tertiary recovery of residual SME in terms of rapid recovery and high recovery efficiency by reducing IFT and generating foam for mobility control.

4. In an oil-wet, layered sandpack with a 34:1 permeability contrast, NIB foam was able to mobilize and recover remaining oil from the lower, low-permeability layer.

References

Aronofsky, J.S., Masse, L. and Natanson, S.G., "A model for the mechanism of oil recovery from the porous matrix due to water invasion in fractured reservoirs," *Trans. AIME* 213, 17-19, 1958.

Austad, T. and Milter, J.: "Spontaneous Imbibition of Water Into Low Permeable Chalk at Different Wettabilities Using Surfactants," paper SPE 37236 presented at the 1997 SPE International Symposium on Oilfield Chemistry, Houston, 18–21 February.

Aveyard, R., Binks, B.P., Fletcher, P.D.I., Peck, T.G., Rutherford, C.E., *Advanced Colloid Interface Science, 48* (1994) 93.

Basheva, E.S., Ganchev, D., Denov, N.D., Kasuga, K., Satoh, N., Tsujii, K. 2000. "Role of Betaine as Foam Booster in the Presence of Silicone Oil Drops," *Langmuir, Vol. 16*, 1000-1013.

Bertin, H.J., Apaydin, O.G., Castanier, L.M., and Kovscek, A.R. 1999. "Foam Flow in Heterogeneous Porous Media: Effect of Crossflow," *SPEJ,* (June 1999): 75-82.

Blaker,T., Aarra, M.G. Skauge, A. Rasmussen, L., Celius, H.K., Martinsen, H.A., Vassenden, F. 2002. "Foam for Gas Mobility Control in the Snorre Field: The FAWAG Project," *SPE Reservoir Evaluation & Engineering, 5* (4): 317-323.

Chen, H.L. *et al.*: "Laboratory Monitoring of Surfactant Imbibition Using Computerized Tomography," paper SPE 59006 presented at the 2000 SPE International Petroleum Conference and Exhibition, Villahermosa, Mexico, 1–3 February.

Christov, N.C., Denkov, N.D., Kralchevsky, P.A., Ananthapadmanabhan, K.P., and Lips, A. 2004. "Synergistic Sphere-to-Rod Micelle Transition in Mixed Solutions of Sodium Dodecyl Sulfate and Cocoamidopropyl Betaine," *Langmuir, 20*, 565-571.

Dake, L.P., *Fundamentals of Reservoir Engineering*, New York: Elsevier, 1978.

Garrett, P.R., “The Mode of Action of Antifoams,” in *Defoaming: Theory and Industrial Applications*, edited by P.R. Garrett, Marcel Dekker, New York, 1993, p. 14.

Gupta, R. and Mohanty, K.K. 2007. “Temperature effects on Surfactant-Aided Imbibition Into fractured Carbonates,” SPE 110204 presented at the SPE ATC&E, Anaheim, CA, 11-14 November.

Hagoort, J.: “Oil Recovery by Gravity Drainage,” *SPEJ* (June 1980) 139.Heller, J.P. 1994. “CO2 Foam in Enhanced Oil Recovery,” in Schramm, L.L., Foams: Fundamentals and Applications in the Petroleum Industry, American Chemical Society, Washington, DC.

Hirasaki, G. J., "Sensitivity Coefficients for History Matching Oil Displacement Processes", *SPEJ* (February 1975), 39-50.

Hirasaki, G.J. 1989. “The Steam-Foam Process,” *J. Pet. Tech.* (May 1989): 449-456.

Hirasaki, G.J., Miller, C.A., Szafranski, R., Tanzil, D., Lawson, J.B., Meinardus, H., Jin, M., Londergan, J.T., Jackson, R.E., Pope, G.A., and Wade, W.H. 1997. “Field Demonstration of the Surfactant/Foam Process for Aquifer Remediation,” SPE 39292 prepared for presentation at the 1997 SPE ATCE in San Antonio, TX, 5-8 October.

Hirasaki, G.J., Jackson, R.E., Jin, M., Lawson, J.B., Londergan, J., Meinardus, H., Miller, C.A., Pope, G.A., Szafranski, R., and Tanzil, D. 2000. “Field Demonstration of the Surfactant/Foam Process for Remediation of a Heterogeneous Aquifer Contaminated with DNAPL,” *NAPL Removal: Surfactants, Foams, and Microemulsions*, S. Fiorenza, C.A. Miller, C.L. Oubre, and C.H. Ward, ed., Lewis Publishers.

Hirasaki, G.J., Zhang D.L.: “Surface Chemistry of Oil Recovery From Fractured, Oil-Wet, Carbonate Formations,” *SPEJ*., (June 2004) SPE 88365-PA.

Hjelmeland, O. and Larrondo, L.E.: “Experimental Investigation of the Effects of Temperature, Pressure, and Crude Oil Composition on Interfacial Properties,” *SPERE* (July 1986) 321-328.

Kovscek, A.R. and Bertin, H. J., " Foam Mobility in Heterogeneous Porous Media I: Scaling Concepts," *Transport in Porous Media*, 52, 17-35 (2003).

Kovscek, A.R. and Bertin, H. J, " Foam Mobility in Heterogeneous Porous Media II: Experimental Observations," *Transport in Porous Media*, 52, 37-49 (2003).

Lawson, J.B., Reisberg, J., 1980. “Alternate Slugs of Gas and Dilute Surfactant for Mobility Control during Chemical Flooding,” SPE 8839 presented at the SPE/DOE Enhanced Oil Recovery Symposium, 20-23 April, Tulsa, Oklahoma.

Li, R.F., Yan, W., Liu, S., Hirasaki, G.J., and Miller, C.A.: “Foam Mobility Control for Surfactant Enhanced Oil Recovery,” *SPE J*. (December 2010) SPE-113910-PA.

Li, R.F., “Study of Foam Mobility Control in Surfactant Enhanced Oil Recovery Processes in 1-D, Heterogeneous 2-D, and Micro Model Systems,” Ph.D. Thesis, Rice University, Houston TX, 2011.

Ma, S., Morrow, N.R. and Zhang, X., “Generalized scaling of spontaneous imbibition. data for strongly water-wet systems,” *J. Pet. Sci. & Eng.* 18 (1997) 165-178.

Manlowe, D.J. and Radke, C.J. 1990. “A Pore-Level Investigation of Foam/Oil Interactions in Porous Media,” *SPE Reservoir Engineering, 5* (4): 495-502.

Masalmeh, S.K., Oedai, S., “Surfactant Enhanced Gravity Drainage: Laboratory Experiments and Numerical Simulation Model,” SCA2009-06, presented at the International Symposium of the Society of Core Analysts, September, 2009.

Masalmeh, S.K., Wei, L.: “EOR Option for a Heterogeneous Carbonate Reservoirs with Complex Waterflood Performance,” 15th European Symposium on Improved Oil Recovery, April 2009.

Morrow, N.R.: “Wettability and Its Effect on Oil Recovery,” *JPT*, (December 1990) 1476-1484.

Nikolov, A.D., Wasan, D.T., Huang, D.W., Edwards, D.A. 1986. The Effect of Oil on Foam Stability: Mechanisms and Implications for Oil Displacement by Foam in Porous Media. SPE 15443 presented at the SPE ATCE, 5-8 October, New Orleans, Louisiana.

Nguyen, Q.P., Currie, P.K., Zitha, P.L.J. 2005. “Effect of Crossflow on Foam-Induced Diversion in Layered Formations,” *SPEJ,* (March 2005): 54-65.

Patzek, T.W. 1996. “Field Application of Steam Foam for Mobility Improvement and Profile Control,” *SPE RE, 11*, 79-85.

Pope, G.A., Wu, W., Narayanaswamy, G., Delshad, M., Sharma, M.M., Wang, P., 2000. “Modeling Relative Permeability Effects in Gas-Condensate Reservoirs with a New Trapping Model,” *SPE Reservoir Eval. and Eng*. 2000 3(2) 171-178.

Richardson, J.G. and Blackwell, R.J.: “Use of Simple Mathematical Models for Predicting Reservoir Behavior,” JPT (September 19711145; *Trans., AIME*, 251.

Standnes, D.C. and Austad, T., “ Wettability Alteration in Chalk 2. Mechanism for Wettability Alteration from Oil-Wet to Water-Wet Using Surfactants*,” J. of Pet. Sci. and Eng*., 28 (2000) 123-143.

Treiber, L.E., Archer, D.L., and Owens, W.W.: “A Laboratory Evaluation of the Wettability of Fifty Oil-Producing Reservoirs,” *SPEJ* (December 1972), 531-540.

Yang S.Y, Hirasaki, G.J., Basu, S., Vaidya R.: “Mechanisms for Contact Angle Hysteresis and Advancing Contact Angles,” *J of Petro Sci & Eng 24* (1999) 63-73.

Schramm, L.L., *Emulsions, Foams, and Suspensions: Fundamentals and Applications*, Wiley-VCH: Weinheim, 2005.

Wang, D., Cheng, J., Yang, Z., Li, Q., Wu, W., Yu, H. 2001. “Successful Field Test of the First Ultra-Low Interfacial Tension Foam Flood,” SPE 72147 presented at the SPE Asia Pacific Improved Oil Recovery Conference, 6-9 October, Kuala Lumpur, Malaysia.

Zhang, D., Liu, S., Puerto, M., Miller, C., Hirasaki, G., 2006, “Wettability alteration and spontaneous imbibitions in oil-wet carbonate formations,” *J. Pet. Sci. & Eng., 52*, 213-226.

Zhang, H., Miller, C.A., Garrett, P.R., Raney, K.H., *Journal of Colloid and Interface Science, 263* (2003) 633-644.

Acknowledgment

The financial support of Shell International E&P B.V. is gratefully acknowledged. Shell is also acknowledged for donation of the 2-D sandpack and the glass micro model.

Author Biographies

Robert F. Li is currently working for Shell International E&P Inc. in Houston TX as an associate research engineer. He received his Ph.D. in Chemical Engineering from Rice University in 2011. His thesis advisors were Prof. George J. Hirasaki, and Prof. Clarence A. Miller. While at Rice, his research topic was surfactant EOR and foam mobility control. He holds his B.S. in Chemical Engineering from Zhejiang University, China.

George J. Hirasaki received a B.S. in Chemical Engineering (1963) from Lamar University and a Ph.D. in Chemical Engineering (1967) from Rice University. He had a 26-year career with Shell Development and Shell Oil Companies before joining the Chemical Engineering faculty at Rice University in 1993. At Shell, his research areas were reservoir simulation, enhanced oil recovery, and formation evaluation. At Rice, his research interests are in NMR well logging, reservoir wettability, enhanced oil recovery, gas hydrate recovery, asphaltene deposition, emulsion coalescence, and surfactant/foam aquifer remediation. He received the SPE Lester Uren Award in 1989. He was named an Improved Oil Recovery Pioneer at the 1998 SPE/DOR IOR Symposium. He was the 1999 recipient of the Society of Core Analysts Technical Achievement Award. He is a member of the National Academy of Engineers.

Clarence A. Miller is Louis Calder Professor Emeritus of Chemical and Biomolecular Engineering at Rice University and a former chairman of the department. His B.S. and Ph.D. degrees were from Rice (1961) and the University of Minnesota (1969), both in chemical engineering. Before coming to Rice he taught at Carnegie-Mellon University. He has been a Visiting Scholar at Cambridge University, the University of Bayreuth (Germany), and Delft University of Technology (Netherlands). His research interests center on emulsions, microemulsions, and foams and their applications in detergency, enhanced oil recovery, and aquifer remediation. He is coauthor of the book *Interfacial Phenomena,* now in its second edition.

Shehadeh Masalmeh is currently working as a principle EOR reservoir engineer with Shell. He has a B.Sc. (1990) in physics from Birzeit University, Palestine. He obtained an M.Sc. in atomic physics from the University of Amsterdam and a Ph.D. in Quantum Optics from the University of Leiden in 1997. In his current position, he is leading and actively working in several EOR research projects. Masalmeh joined Shell in 1997 where he worked in the SCAL team and since then moved into several international assignments where he worked on field development studies, sour gas fields and EOR. His research interests include fluid flow in porous media, rock typing, wettability, hysteresis, transition zone, Chemical and Gas EOR. Masalmeh has authored and co-authored more than 35 papers for symposiums and journals and he has several patents.

Figure Captions

Fig. 1— Photograph of 2-D heterogeneous sandpack. Black arrows show direction of flow through manifolds. Red arrows identify different sand layers.

Fig. 2—Water receding and advancing contact angles with oil on glass in 2% NaCl brine.

Fig. 3—Photograph after oilflood. Initial oil saturation 62.4%. The arrow indicates flow direction.

Fig. 4—Photograph after 4.0 PV waterflood. Remaining oil saturation 31.8%. The arrow indicates flow direction.

Fig. 5—Photographs of gravity driven counter-current flow during shut-in.

Fig. 6— Recovery as a function of dimensionless times. The adverse capillary pressure dominated gravity and retarded recovery by buoyancy. The rate limiting step was the transport of the surfactants to the trapped oil.

Fig. 7—Foamflood profiles. The arrow shows the direction of flow. Notice the patch of remaining oil near the inlet moved upward instead of forward. This is another evident of the presence of water-in-oil emulsion in this patch of oil because of the yield stress attributed to the emulsion.

Fig. 8—Apparent viscosity during the foamflood. Lowest points indicate when air was injected. Higher two rows of points indicate when IOS 15-18 was injected.

Fig. 9—Photographs after the foamflood. Gravity and capillary pressure driven counter-current flow was observed immediately after foamflood when the system was shut in.

Fig. 10—Effluent samples from the foamflood.

Fig. 11—Summary of cumulative oil recovery and oil-cut. Shut-in occurred after NI injection at 4.5 TPV.

Fig. 12—Comparison of foaming ability among NI, AOS 16-18, and NIB. NI foam was injected at 0.5 psi/ft with

fg=0.5. NIB and AOS 16-18 were injected at 20 ft/D with *fg*=2/3.

Fig. 13—NI alone without lauryl betaine in presence of SME in a glass micro model.

Fig. 14—NIB (NI:lauryl betaine=1:2) in presence of SME in a glass micro model.

Fig. 15—Cumulative recovery curves of waterflood residual oil in experiments (a) and (b).

Fig. 16—Foam apparent viscosity curves in experiments (a) and (b).

Fig. 17—Displacement profiles and pictures of effluent in experiment (a). The sandpack was oriented vertically. The arrow indicates the direction of flow from bottom to top.

Fig. 18—Displacement profiles and pictures of effluent in experiment (b). The sandpack was oriented vertically. The arrow indicates the direction of flow.

Fig. 19—Viscosity with IOS15-18 and lauryl betaine blends in 1% Na_2CO_3 and 3.5% NaCl.

Fig. 20—Qualitative NIB foam stability test. All vials contained 0.5% lauryl betaine (except NI only) in 1% Na_2CO_3 and 3.5% NaCl. All bottles were manually shaken continuously for 10 minutes. Pictures were taken 15 minutes after shaking. Red boxes highlight the presence of (strong) foam on top of bulk solution with and without the presence of crude oil.

Fig. 21—Displacement profiles and pictures of effluent in an ASF process using NIB alone. The sandpack was oriented vertically. The arrow indicates the direction of flow.

Fig. 22—Cumulative recovery curves with NIB alone in a tertiary recovery process of residual SME.

Fig. 23—Foam apparent viscosity during the ASF process using NIB alone.

Fig. 24—Injection rate during the ASF process using NIB alone.

Fig. 25—Foam using NIB alone in a secondary recovery. Flow direction was vertical.

Fig. 26—Cumulative recovery curves using NIB alone in a secondary recovery process of SME crude. The sandpack was oriented vertically. The arrow indicates the direction of flow.

Fig. 27—Photographs during waterflood in the oil-wet sand column. Lower layer remained highly oil-saturated because of wettability (oil-wet) and lower permeability. The sandpack was oriented horizontally. The arrow indicates the direction of flow.

Fig. 28—Photographs during ASF process in the oil-wet sand column. The sandpack was oriented horizontally. The arrow indicates the direction of flow.

Fig. 29—Foam apparent viscosity during the ASF process in the oil-wet sand column.

Table 1. List of Materials

Name	*Description*
Neodol 67-7PO	ammonium C16-17 7PO sulfate, *Stepan*
IOS 15-18	sodium 15-18 internal olefin sulfonate, *Shell*
AOS 16-18	sodium 16-18 alpha olefin sulfonate, *Stepan*
Lauryl Betaine	a zwitterionic surfactant used as a foam booster, *Rhodia*
NI	a blend of 4:1 (wt/wt) Neodol 67-7PO and IOS 15-18 used to alter the wettability and/or lower the IFT
NIB	a blend of 4:1:10 (wt/wt/wt) Neodol 67-7PO, IOS 15-18 and lauryl betaine unless otherwise stated; used to lower the IFT and generating strong foam in presence of crude oil
IB	a blend of IOS 15-18 and lauryl betaine used to generate foam in presence of crude oil
CTAB	hexadecyltrimethylammonium bromide used to change the wettability of natural clean silica from water-wet to oil-wet, *Matheson Coleman & Bell*
SME (code name) Crude Oil	API=41.1°, 3.93 cp at 25°C, Total acid number (TAN) = 0.062 mgKOH/g
Silica Sand Oil Frac 20/40	coarse grain sand, ~88~ 200 darcy, *U.S. Silica Co.*
Silica Sand F-110	fine grain sand, ~ 4.8 darcy, *U.S. Silica Co.*
Silica Flour	MIN-U-SIL 30, *U.S. Silica Co.*
Na_2CO_3	anhydrous, certified American Chemical Society , used as alkaline in the ASF slug, *Fisher Scientific*
NaCl	biological certified, *Fisher Scientific*

Table 2. Types of Glass Slides and Their Surface Properties

Type of Glass	*Surface Treatment*	*Wettability*
Clean Glass	Untreated glass to mimic the natural state of silica surface.	water-wet
CTAB-Treated Glass	Clean glass slides mentioned above soaked in CTAB (~ ½ CMC) solution for 20 minutes, and rinsed with sufficient deionized water before use.	oil-wet
CTAB- Then NI-Treated Glass:	CTAB-treated glass slides as above soaked in NI for 20 minutes and rinsed with sufficient deionized water before use.	water-wet

Table 3. Summary of 2-D CTAB-treated SME ASF Flood

2-D Sand Pack	**CTAB-treated silica, coarse sand overlays fine sand; porosity 0.38; thickness ratio 2:3; permeability ratio 19:1; overall permeability 44 darcy; PV 330 mL;**
Oilflood	**1.5 PV oil; 5-10 ft/D; Oil saturation: 62.4%;**
Waterflood (2% NaCl)	**4 PV (5 ft/D, ~0.06 psi/ft) cumulative recovery 49.1% OOIP; remaining oil saturation 31.8%;**
Chemical Slugs	**surfactant 0.2% NI in 1% Na_2CO_3, 2% NaCl; foam drive 0.5% IOS15-18 in 1% Na_2CO_3, 2% NaCl;**
Injection Scheme	**0.5 PV NI (1 ft/D); cumulative recovery 51.5% OOIP; remaining oil saturation 30.3%; shut-in for 42 days; 0.1 PV IOS (1 ft/D)→0.1 PV IOS (1 ft/D)→0.1PV Air (1.6 psi/ft); 0.1 PV IOS (1.6 psi/ft)→0.1 PV IOS (1.6 psi/ft)→0.1PV Air (1.6 psi/ft); etc.; cumulative recovery 94.6% of OOIP; remaining oil saturation 3.4%.**

Table 4. Summary of two experiments in 1-D homogeneous sandpacks

Experiments	(a) NI and IOS	(b) NIB and IB
Silica Sand Pack	142 darcy	193 darcy
Flow Direction	Vertical	Vertical
Surfactant Concentration (wt%)	NI (0.16% N67-7PO, 0.04% IOS15-18	NIB (0.2% N67-7PO, 0.05% IOS15-18, 0.5% lauryl betaine)
Foam Drive (wt%)	0.5% IOS 15-18	IB (0.5% IOS15-18, 0.05% lauryl betaine)
Salinity	1% Na_2CO_3, 2% NaCl	1% Na_2CO_3, 3.5% NaCl
Residual Oil Saturation after Waterflood	26.4%	20.9%
Surfactant Slug	0.3 PV NI	0.3 PV NIB
Injection Scheme	1.2 psi/ft	5 ft/D NIB (0-0.2TPV); 1.4 psi/ft from 0.3th TPV.
Foam Generation	SAG, *fg*=0.5	SAG, *fg*=0.5
Oil Breakthrough	1.1 TPV	0.7 TPV
Cumulative Recovery of Residual Oil	98.6% at 2.3 TPV	99.7% at 1.9 TPV

Table 5. Summary of the foam experiment in an oil-wet heterogeneous sand column

	Oil-Wet Column
Sandpack	43 darcy, coarse overlays fine sand
Flow Direction	horizontal
Surfactant Formulation	NIB, 1.18 cp
Salinity	3.5% NaCl, 1% Na_2CO_3
Temperature	25 °C
Oil Viscosity	3.93 cp (25°C)
Injection Scheme	5 ft/D (0-0.2TPV); 2.5 psi/ft from 0.3 TPV
Slug Size	0.1 PV
Foam Generation	NIB alternating air; *fg*=1/3
Initial Oil Saturation	S_{oi}=1
Waterflood Remaining Oil Saturation	S_{orw}=0.62
(Incremental Recovered Oil by EOR/ Waterflood Remaining Oil)x100%	88.7%
Cumulative Recovery (Waterflood+EOR)	93.1%

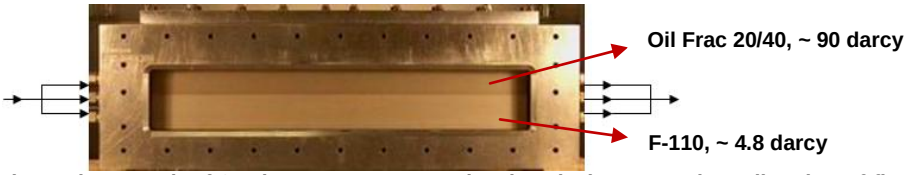

Fig. 1 Photograph of 2-D heterogeneous sandpack. Black arrows show direction of flow through manifolds. Red arrows identify different sand layers.

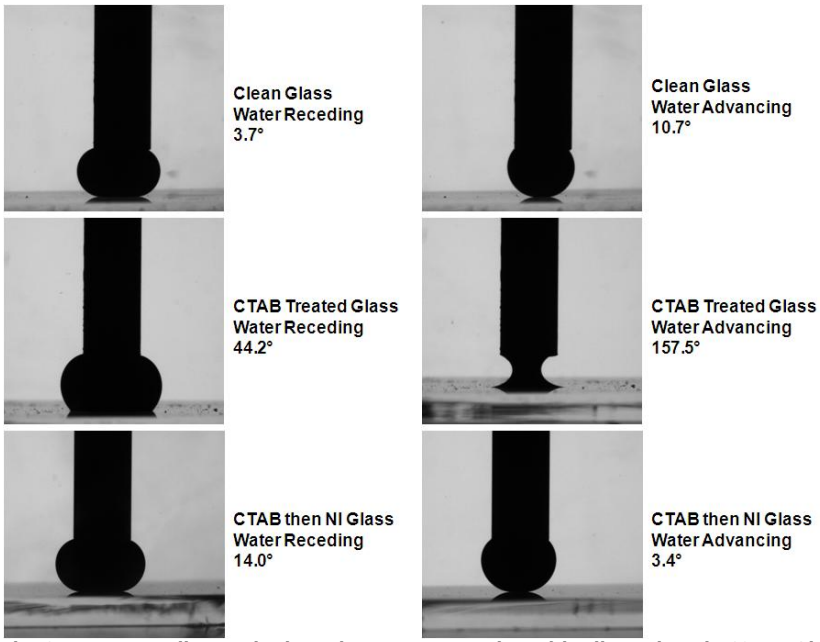

Fig. 2 Water receding and advancing contact angles with oil on glass in 2% NaCl brine.

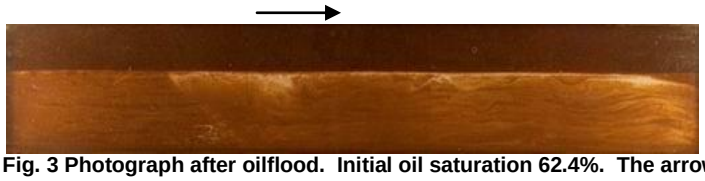

Fig. 3 Photograph after oilflood. Initial oil saturation 62.4%. The arrow indicates flow direction.

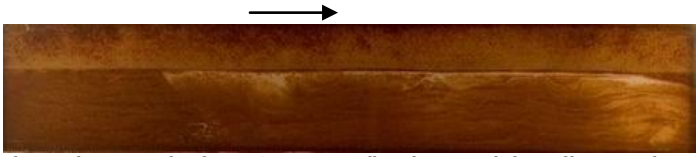

Fig. 4 Photograph after 4.0 PV waterflood. Remaining oil saturation 31.8%. The arrow indicates flow direction.

Displacement Profiles during System shut-in	t (day)	t_{Dg}	$t_{D,\,Pc}$
	0	0	0
	2	53	0.5
	6	107	1.0
	10	178	1.6
	42	748	6.7

Fig. 5 Photographs of gravity-driven counter-current flow during shut-in.

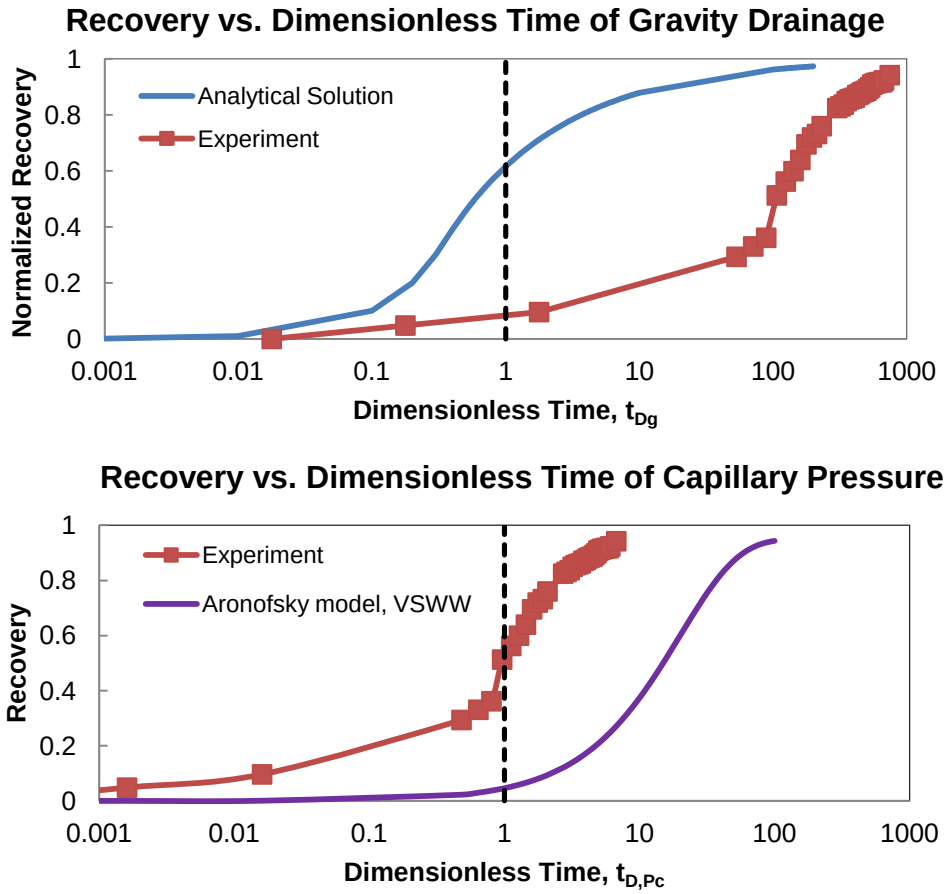

Fig. 6 Recovery as a function of dimensionless times. The adverse capillary pressure dominated gravity and retarded recovery by buoyancy. The rate limiting step was the transport of the surfactants to the trapped oil.

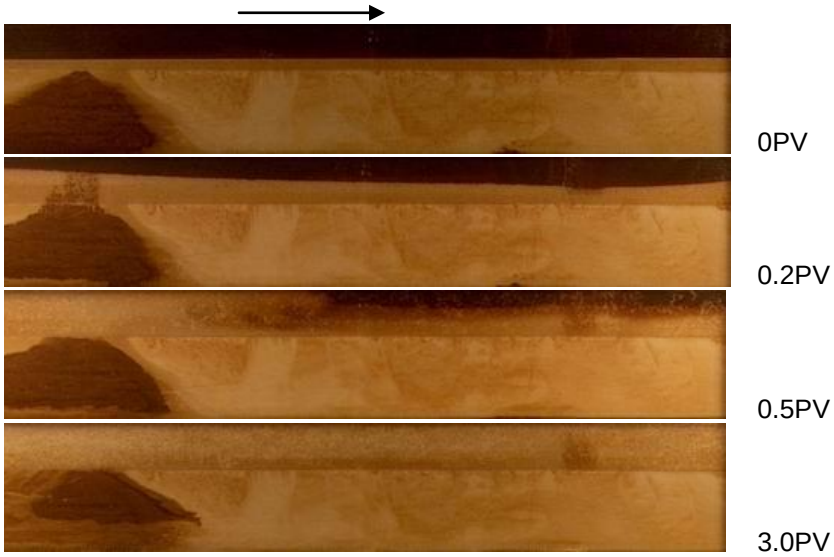

Fig. 7 Foamflood profiles. The arrow shows the direction of flow. Notice the patch of remaining oil near the inlet moved upward instead of forward. This is another evident of the presence of water-in-oil emulsion in this patch of oil because of the yield stress attributed to the emulsion.

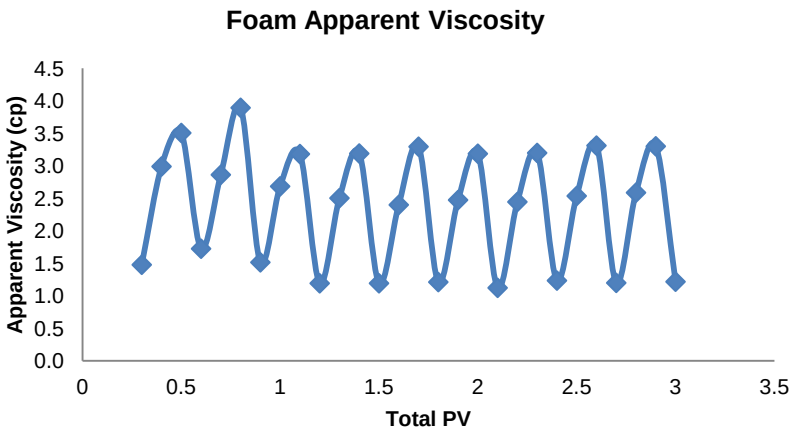

Fig. 8 Apparent viscosity during the foamflood. Lowest points indicate when air was injected. Higher two rows of points indicate when IOS 15-18 was injected.

Fig. 9 Photographs after the foamflood. Gravity and capillary pressure driven counter-current flow was observed immediately after the foamflood when the system was shut in.

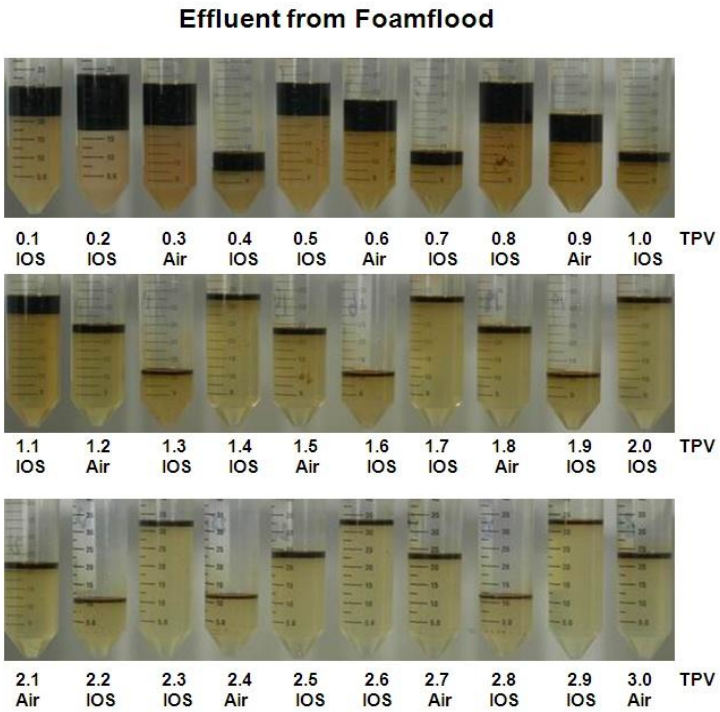

Fig. 10 Effluent samples from the foamflood.

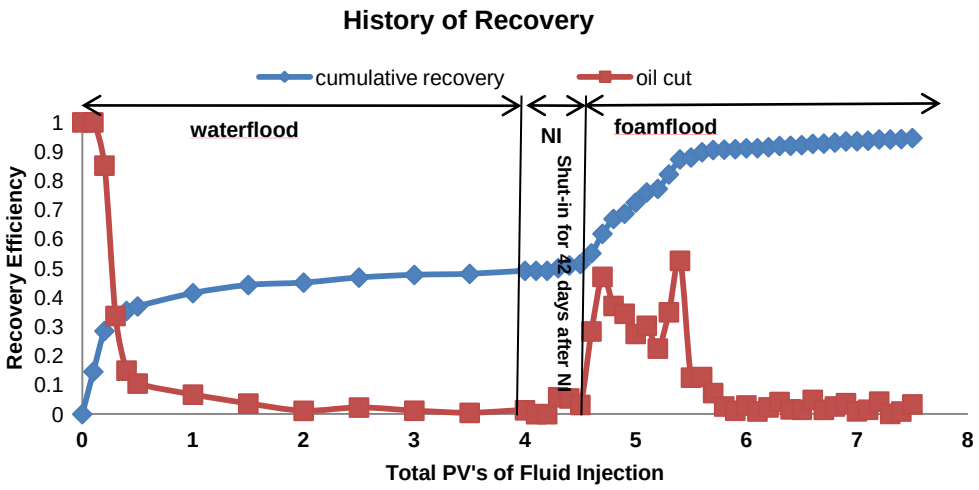

Fig. 11 Summary of cumulative oil recovery and oil-cut. Shut-in occurred after NI injection at 4.5 TPV.

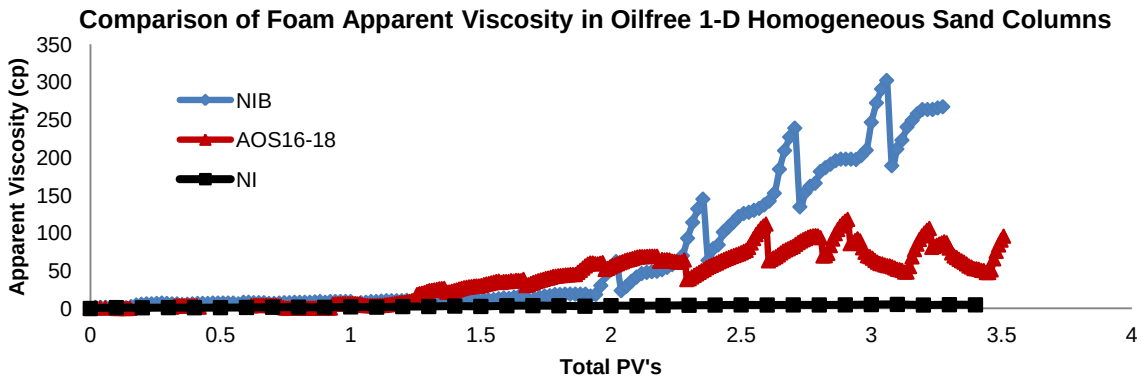

Fig. 12 Comparison of foaming ability among NI, AOS 16-18, and NIB. NI foam was injected at 0.5 psi/ft with *fg*=0.5. NIB and AOS 16-18 were injected at 20 ft/D with *fg*=2/3.

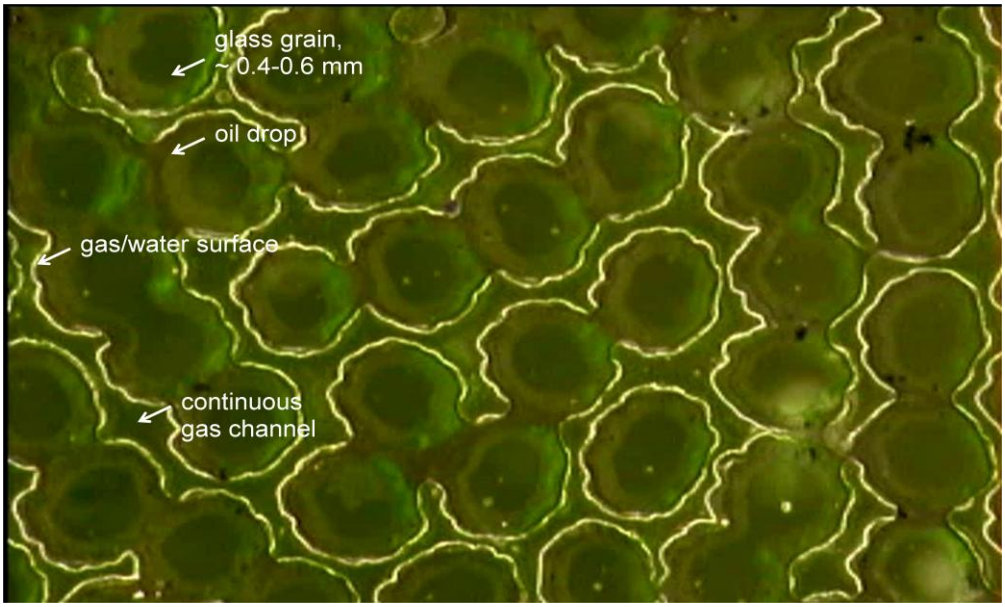

Fig. 13 NI alone without lauryl betaine in presence of SME in a glass micro model.

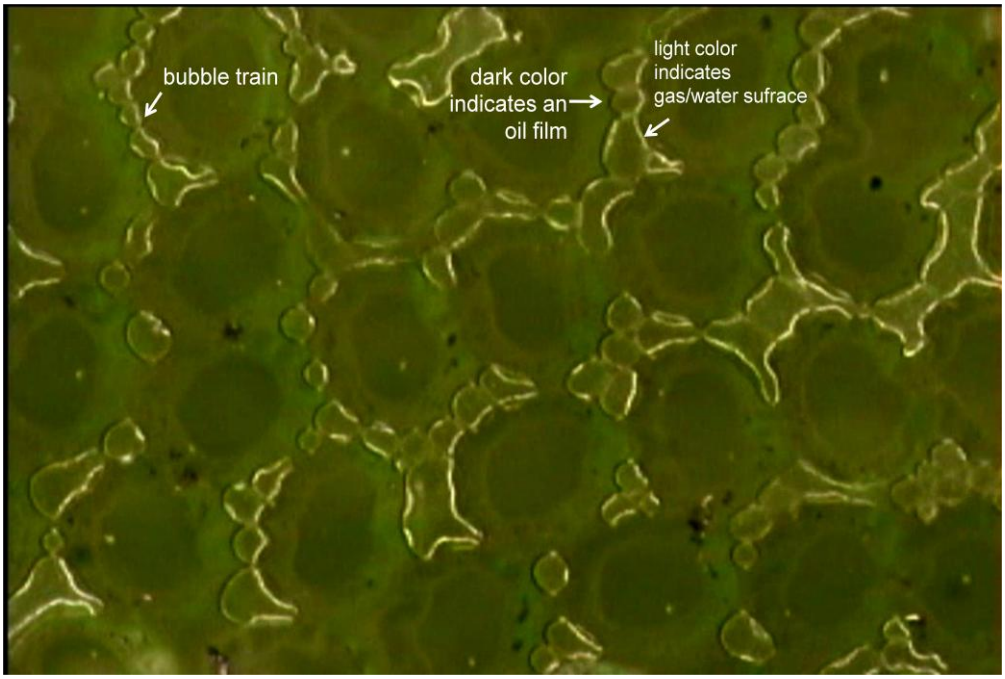

Fig. 14 NIB (NI:lauryl betaine=1:2) in presence of SME in a glass micro model.

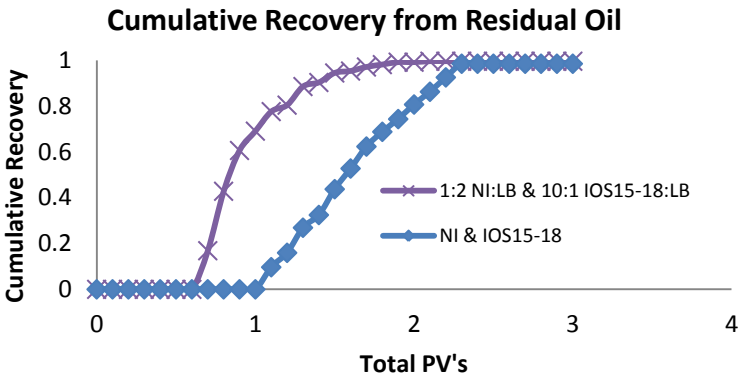

Fig. 15 Cumulative recovery curves of waterflood residual oil in experiments (a) and (b).

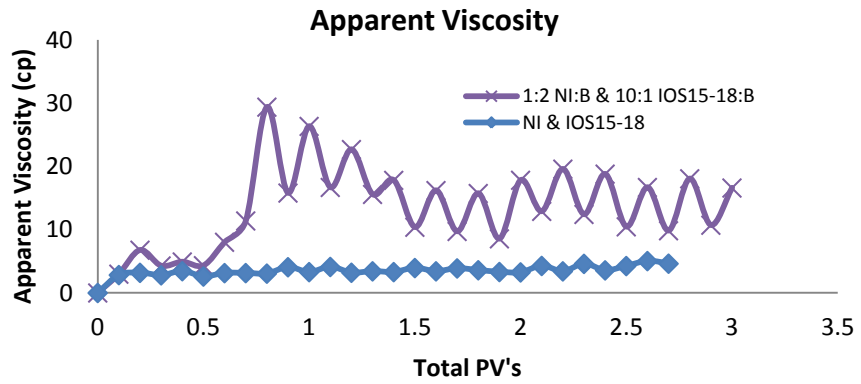

Fig. 16 Foam apparent viscosity curves in experiments (a) and (b).

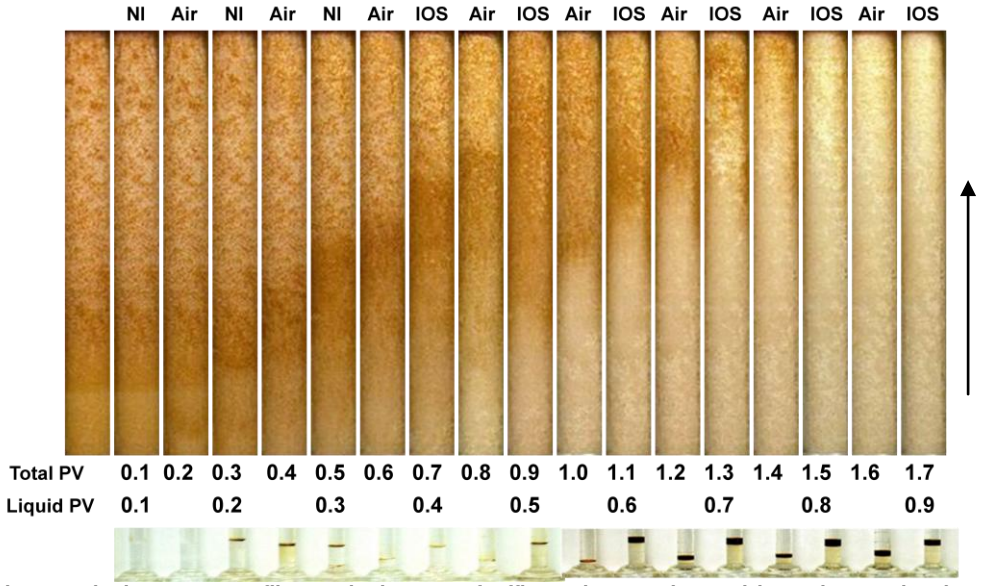

Fig. 17 Displacement profiles and pictures of effluent in experiment (a). The sandpack was oriented vertically. The arrow indicates the direction of flow from bottom to top.

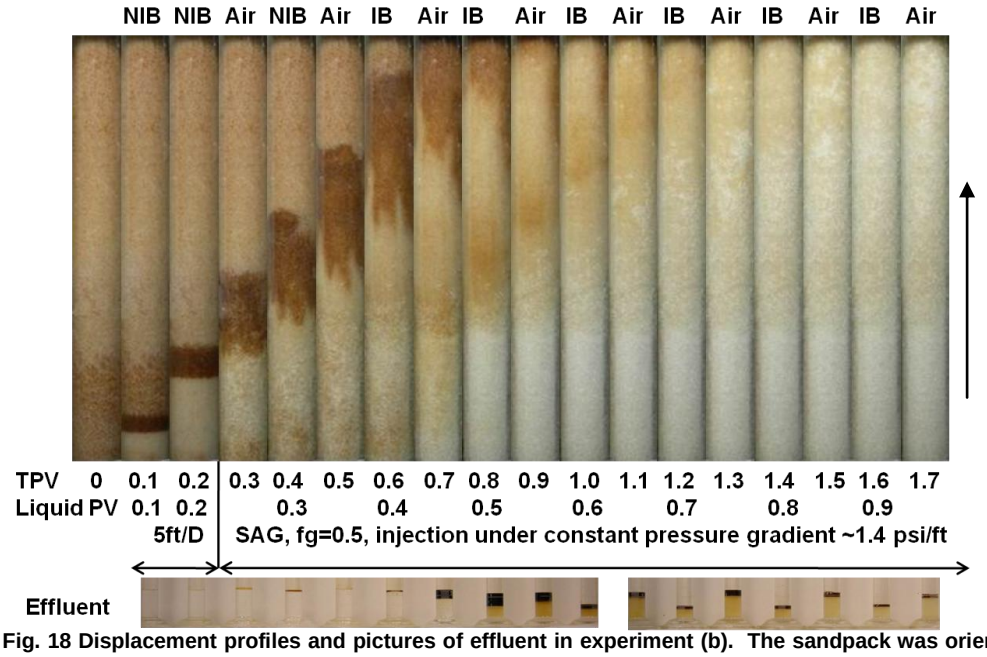

Fig. 18 Displacement profiles and pictures of effluent in experiment (b). The sandpack was oriented vertically. The arrow indicates the direction of flow.

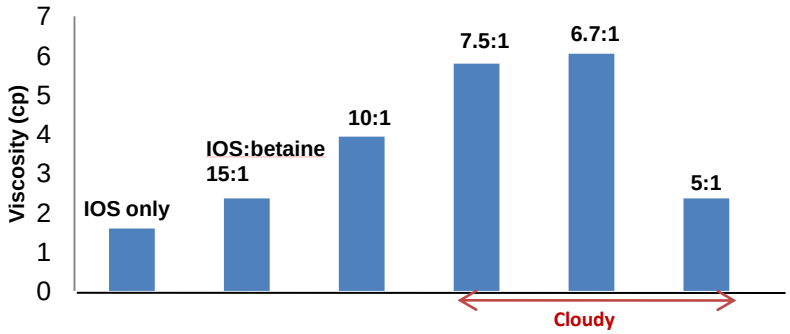

Fig. 19 Viscosity with IOS15-18 and lauryl betaine blends in 1% Na_2CO_3 and 3.5% NaCl.

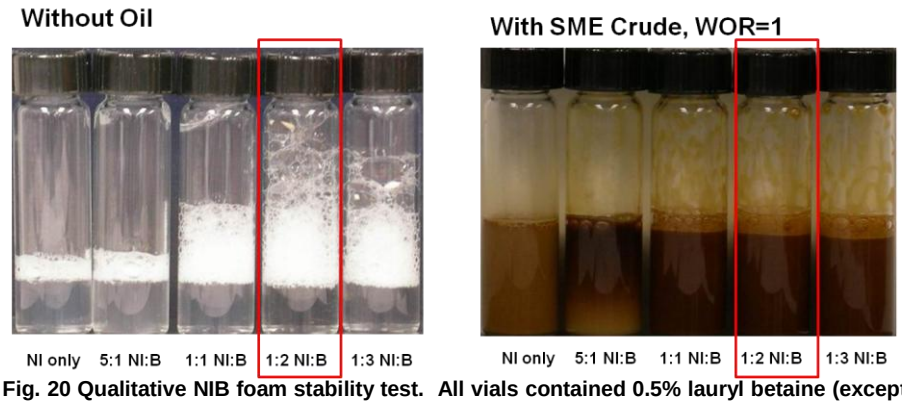

Fig. 20 Qualitative NIB foam stability test. All vials contained 0.5% lauryl betaine (except NI only) in 1% Na_2CO_3 and 3.5% NaCl. All bottles were manually shaken continuously for 10 minutes. Pictures were taken 15 minutes after shaking. Red boxes highlight the presence of (strong) foam on top of bulk solution with and without the presence of crude oil.

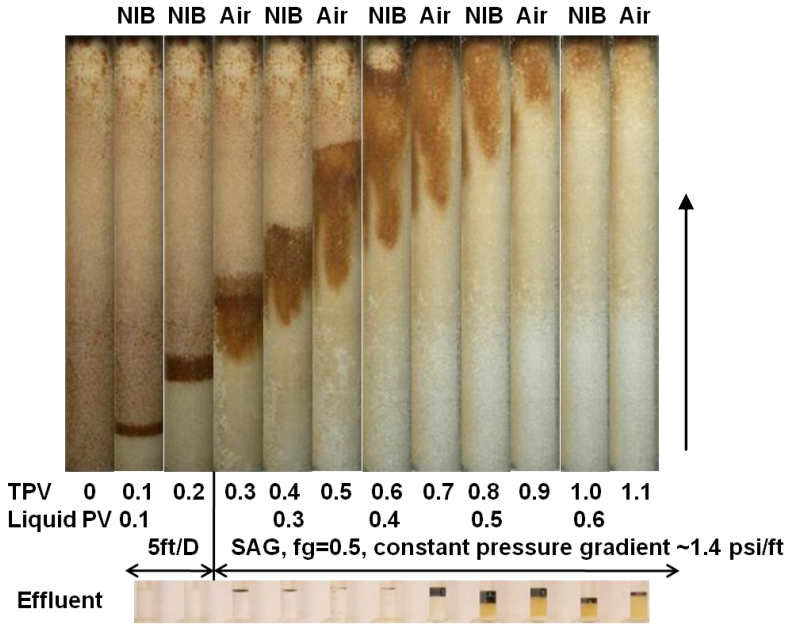

Fig. 21 Displacement profiles and pictures of effluent in an ASF process using NIB alone. The sandpack was oriented vertically. The arrow indicates the direction of flow.

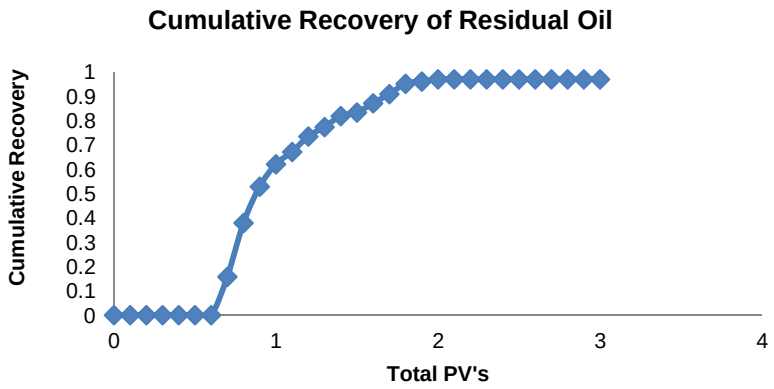

Fig. 22 Cumulative recovery curves with NIB alone in a tertiary recovery process of residual SME.

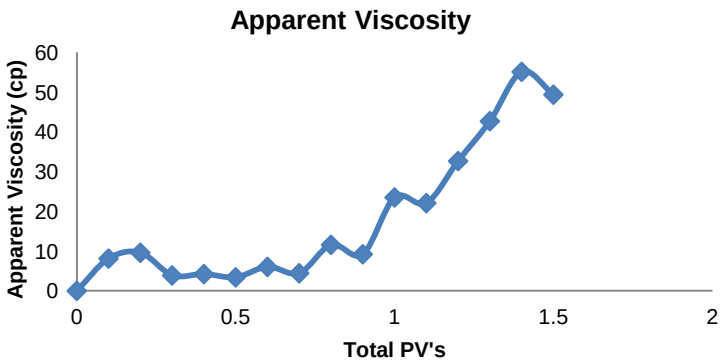

Fig. 23 Foam apparent viscosity during the ASF process using NIB alone.

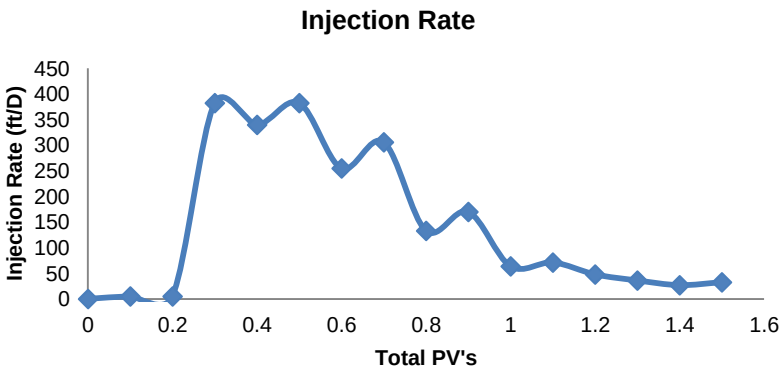

Fig. 24 Injection rate during the ASF process using NIB alone.

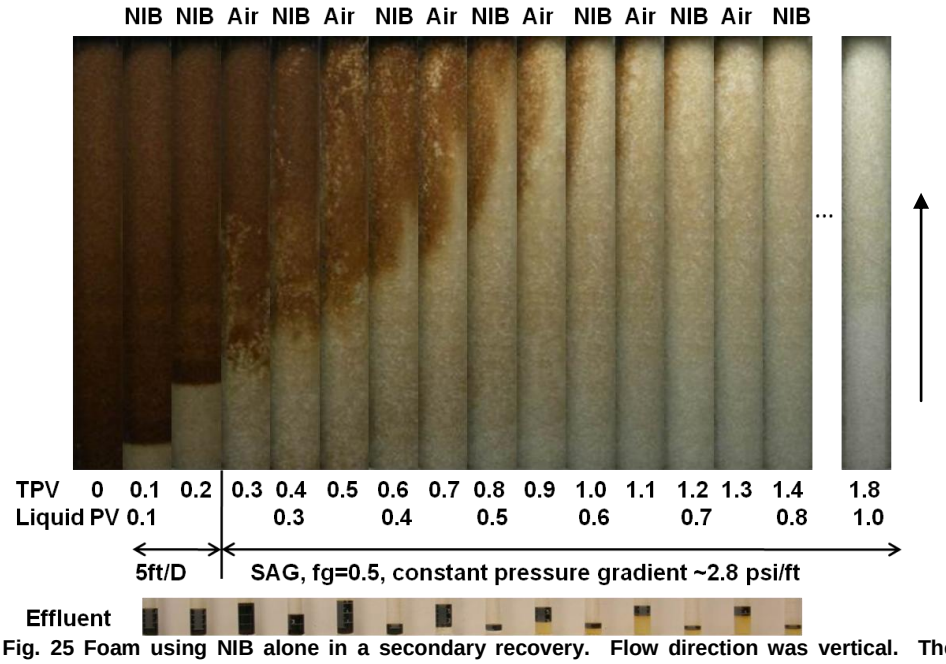

Fig. 25 Foam using NIB alone in a secondary recovery. Flow direction was vertical. The sandpack was oriented vertically. The arrow indicates the direction of flow.

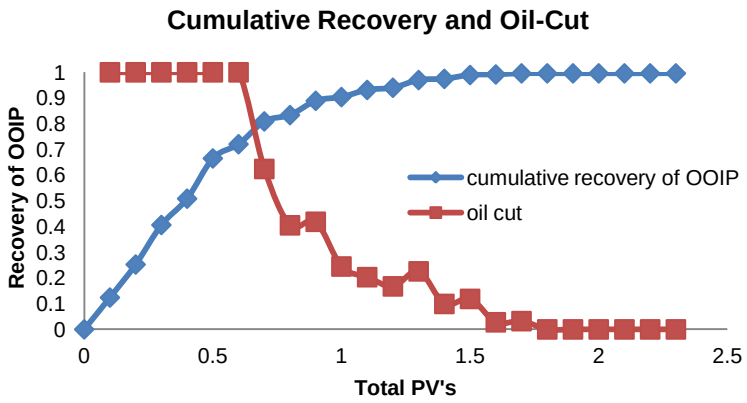

Fig. 26 Cumulative recovery curves using NIB alone in a secondary recovery process of SME crude.

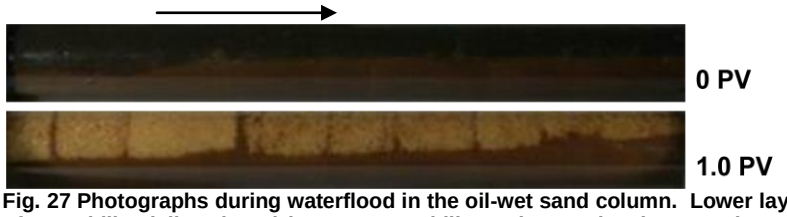

Fig. 27 Photographs during waterflood in the oil-wet sand column. Lower layer remained highly oil-saturated because of wettability (oil-wet) and lower permeability. The sandpack was oriented horizontally. The arrow indicates the direction of flow.

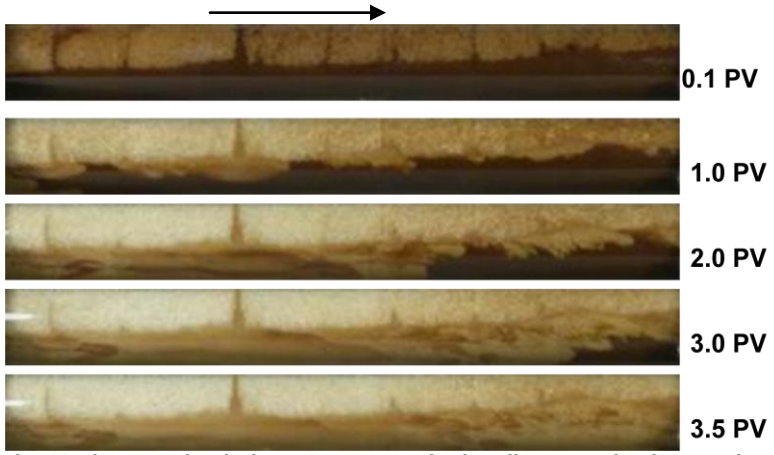

Fig. 28 Photographs during ASF process in the oil-wet sand column. The sandpack was oriented horizontally. The arrow indicates the direction of flow.

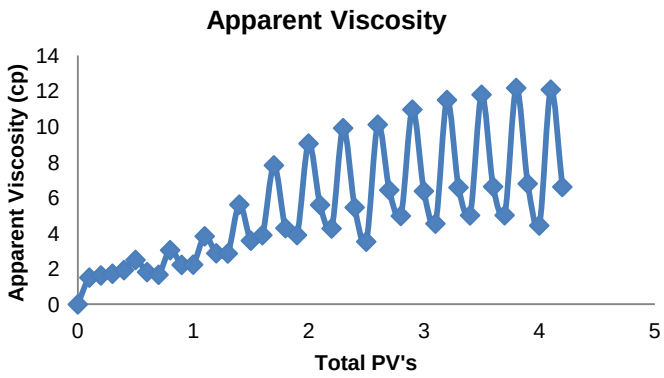

Fig. 29 Foam apparent viscosity during the ASF process in the oil-wet sand column.